SYMMETRIC AND ASYMMETRIC ENHANCEMENT OF POLAR RAIN

Kazuo MAKITA[1] and Ching-I. MENG[2]

[1] Takushoku University, 4-14, Kohinata 3-chome, Bunkyo-ku, Tokyo 113
[2] Applied Physics Laboratory, The Johns Hopkins University,
Johns Hopkins Rd., Laurel, Maryland 20707, U.S.A.

Abstract: From the examination of low-energy electron observed by DMSP-F2, -F3 and -F4 satellites and solar wind data obtained by ISEE-3 satellite, we found that there are two different kinds of polar rain intensification, which are characterized by symmetric and asymmetric enhancement in the two hemispheres, respectively. The intense uniform precipitation of polar rain observed over both hemispheres (symmetric enhancement of polar rain) generally occurs during the period of large IMF fluctuations. This type of precipitation seems to be related to the sudden storm commencement on the ground.

On the other hand, the occurrence of intense polar rain observed in only one hemisphere (asymmetric enhancement of polar rain) depends on the polarity of the IMF *Bx* component. Namely, intense precipitation over the southern polar cap is mostly observed in the positive IMF *Bx* period. On the contrary, when IMF *Bx* is negative, intense precipitation can be seen in the northern polar cap.

1. Introduction

The magnetic field lines which thread the earth's polar caps and extend into lobes of the distant magnetotail are thought to interact directly with the interplanetary magnetic field (IMF) (DUNGEY, 1961; SVALGAARD, 1973; CAMPBELL and MATSUSHITA, 1973). WINNINGHAM and HEIKKILA (1974) showed the existence of very soft (<100 eV) uniform electron precipitation over the entire polar cap called "polar rain". Recently, several people suggested that the sector structure of the IMF shows significant control on the process of this polar rain particle entry and also on the enhancement of the tail lobe plasma. One of the first results of this nature was reported by YEAGER and FRANK (1976). They examined the northern tail-lobe electron fluxes in the hundreds of eV energy range and showed a remarkable correlation with the polarity of the magnetic sector structure in the interplanetary medium; high intensities for the "away" sector and low intensities for the "toward" sector.

These flux increases would be expected to appear in the low-altitude polar cap as well, and this possibility was examined by MENG and KROEHL (1977). They showed that the very intense uniform precipitation of low-energy electron over the northern polar cap was associated with the IMF direction away form the sun and suggested that this kind of intense polar cap electron precipitation may be attributed to the entry of the low-energy solar electrons.

Although the relationship between the polar cap electron precipitation and the IMF sector structure was made clear, the actual IMF measurements during these

examination periods were not available in their analysis. They inferred the IMF polarity by using the ground geomagnetic observations. In order to understand the characteristics of intense low-energy electron precipitation phenomena over the polar cap regions, simultaneous measurements in the low altitude polar region and in the interplanetary space are necessary. In this paper, we analyzed low energy electron precipitations observed by DMSP-F2, -F3 and -F4 satellites and solar wind data observed by ISEE-3 satellite, and examined the control of IMF to the polar cap electron precipitations.

2. Experiments

The precipitating low-energy electron data examined here were obtained by electrostatic analyzers aboard the Air Force operational DMSP-F2, -F3 and -F4 satellites, with an altitude of 840 km and a period of 101.5 min. The electron detector had a field of view of $10° \times 15°$ aligned with the local geocentric zenith and it monitored the precipitating electrons over the polar regions. It measured the precipitations of low-energy electrons between 50 eV and 20 keV in 16 energy channels by using two analyzers (Hardy et al., 1979).

Solar wind data were obtained by ISEE-3 satellite. Since ISEE-3 satellite was located at the distance from the earth of about 250 R_E in this period, the solar wind propagation time between the ISEE-3 satellite position and the earth magnetosphere is estimated to be about one hour. Thus, we used one hour earlier value of IMF and solar wind data, in order to compare them with the low-altitude DMSP satellite data.

3. Symmetric and Asymmetric Enhancement of Polar Rain

From the examination of electron precipitation data, we found that there were two different kinds of intense uniform electron precipitation over the entire polar cap region. One of them is the intense uniform electron precipitation detected in only one hemisphere and another is the intense uniform electron precipitation recognized in both hemispheres. In this chapter, we show examples of these two typical electron precipitation phenomena and discuss the statistical results.

The electron data used in this analysis were obtained in the period from August 12, 1978 to December 31, 1979 with an almost continuous coverage. We have selected the events satisfying the condition that the enhancement of polar rain continued at least 3 hours with the integral electron number flux larger than 8×10^6 (el/cm$^2 \cdot$s$\cdot$sr). We defined the enhancement of polar rain observed in both hemispheres as "symmetric enhancement of polar rain" and the enhancement of polar rain observed in only one hemisphere as "asymmetric enhancement of polar rain".

A typical example of the symmetric enhancement of polar rain is shown in Fig. 1. Top and bottom panels show the electron data obtained in the northern and southern hemispheres, respectively.

In the northern hemisphere, DMSP-F2 satellite traversed over the polar region from the dawn to the dusk sector in the period from 1102 to 1122 UT. Auroral elec-
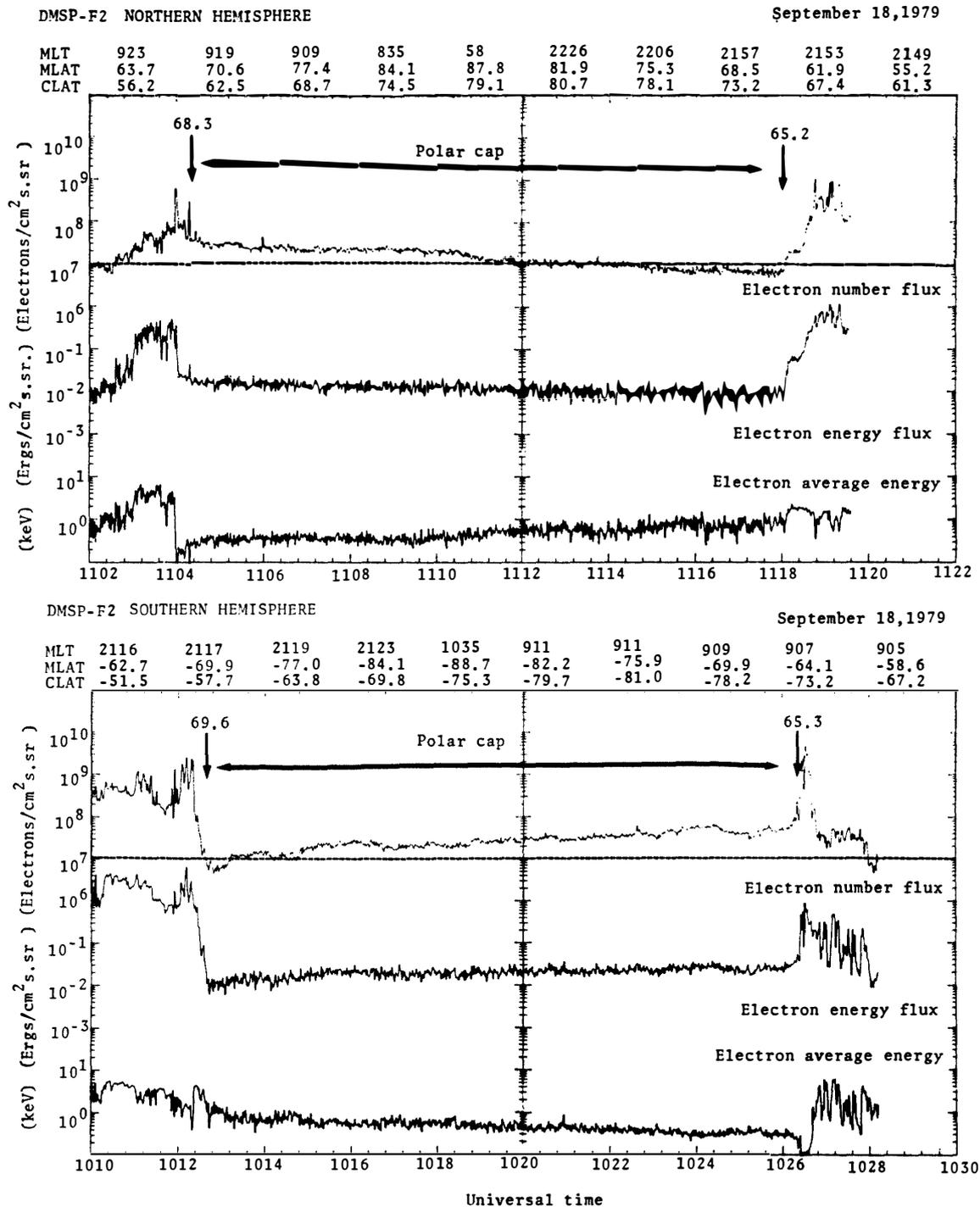
Fig. 1. A typical example of polar rain enhancement observed in both hemispheres. The polar
cap boundaries are seen at 68.3° and 65.2° in the northern hemisphere and 65.3° and 69.6°
in the southern hemisphere. Note that electron number flux in the polar cap regions is
higher than 10^7 $(el/cm^2 \cdot s \cdot sr)$. This value of polar rain flux is larger than that of the
usual polar rain flux by about one order of magnitude.
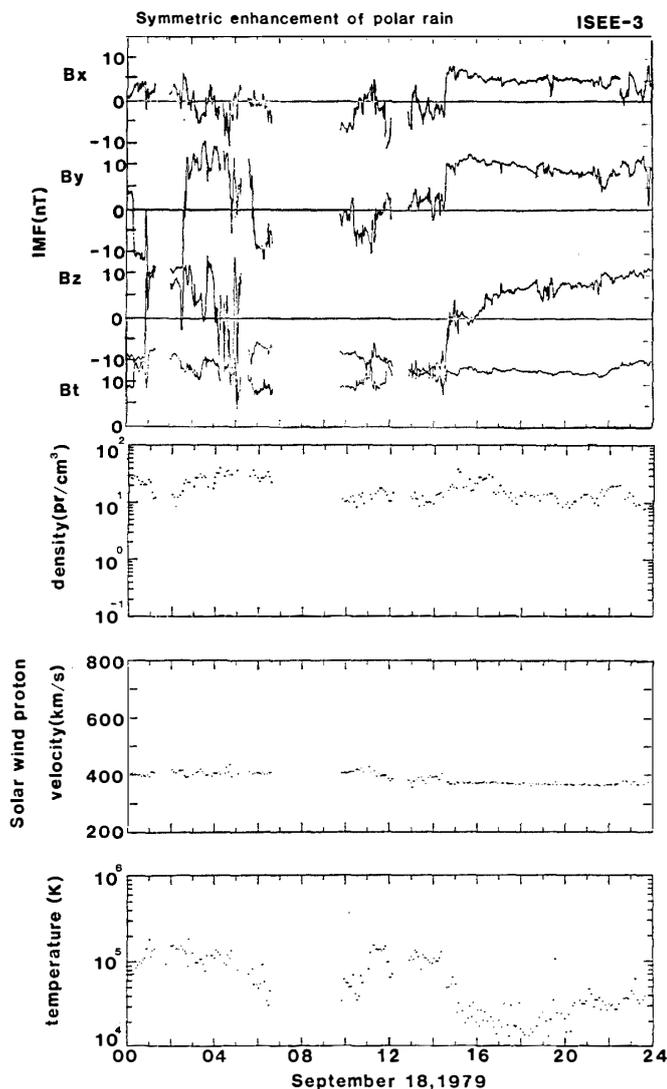
Fig. 2.   IMF and solar wind data obtained by ISEE-3.   Large fluctuation of IMF can be recognized
in this interval.   Solar wind proton density is about 10 (proton/cm^3) and solar wind velocity
is about 400 (km/s).

tron precipitation regions can be recognized on the lower latitude side of 68.3° in the dawn sector and of 65.2° in the dusk sector, respectively.   In the southern hemisphere, DMSP-F2 satellite traversed the polar region from the dusk to the dawn sector in the period from 1010 to 1030 UT.   Precipitation boundaries between the polar cap and the auroral zone can be seen at about 69.6° in the dusk sector and 65.3° in the dawn sector.   This example shows that uniform enhancement of polar rain can be recognized over the polar cap region and the integral electron number flux of the polar rain is larger than 8×10^9 (el/$cm^2 \cdot s \cdot sr$) in both hemispheres.   The enhancement of this polar rain occurred at about 01 UT on September 18 and continued till at about 16 UT on September 18.   Figure 2 shows IMF and solar wind data obtained by ISEE-3 satellite.   The large fluctuation of IMF can be recognized in the period from 00 to 15 UT and an SSC occurred at 0547 UT.   In this interval, the proton density was high (Np=10–30) and
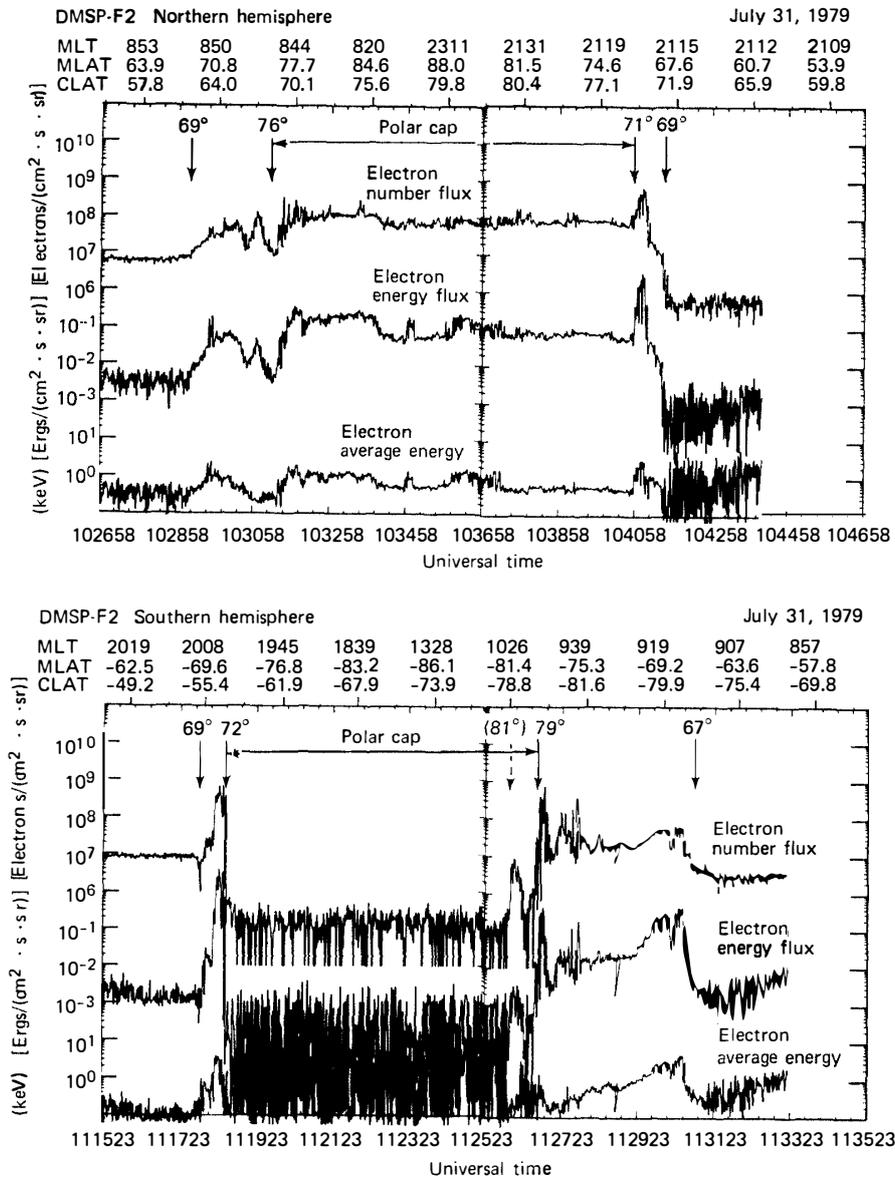
Fig. 3. Typical example of polar rain enhancement observed in only one hemisphere. Enhancement of polar rain flux is about 10^8 ($el/cm^2 \cdot s \cdot sr$). On the other hand, the polar rain flux in the southern hemisphere is extremely low and less than 10^6 ($el/cm^2 \cdot s \cdot sr$).

solar wind velocity was about 400 km/s. More than half of the symmetric enhancement of polar rain examined here was observed after SSC.

On the other hand, the typical asymmetric enhancement of polar rain is shown in Fig. 3. The format in this figure is the same as that in Fig. 1. In the northern hemisphere, the polar cap boundaries are recognized at about 76° in the dawn sector and at 71° in the dusk sector. The polar cap boundaries in the southern hemisphere are seen at about 72° in the dusk sector and at 79° (or 81°) in the dawn sector. It is noted that the enhancement of polar rain can be recognized only in the northern hemisphere. Namely, in the northern hemisphere, the integral number flux was larger than 10^7 ($el/cm^2 \cdot s \cdot sr$), but, the flux in the southern hemisphere was extremely low in this period.
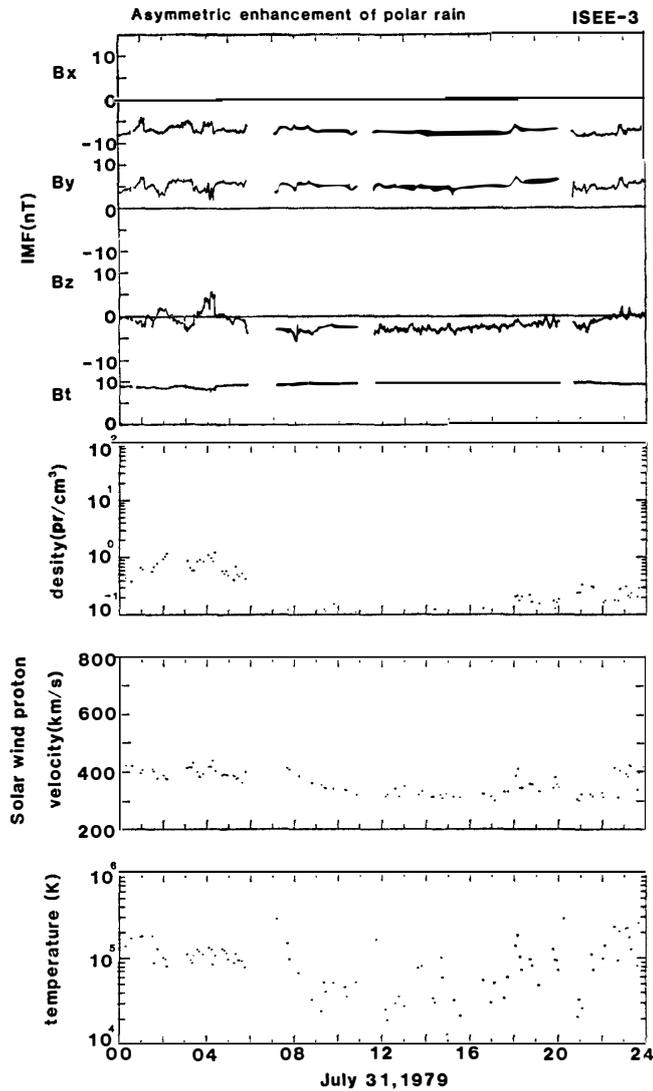
Fig. 4. IMF and solar wind data obtained by ISEE-3.   Note that IMF Bx value is stable and nega-
tive in this interval.   Solar wind proton density is extremely low and solar wind velocity is
between 300–400 (km/s).

The IMF and solar wind data obtained by ISEE-3 satellite are shown in Fig. 4.   The
IMF Bx component was stable and negative in this period.   The proton density was
very low and the solar wind velocity was about 300–400 km/s in this period.   We
examined many other examples and found that asymmetric enhancement of polar
rain frequently occurred during these stable IMF Bx periods.

In order to study the statistical relationship between these two different kinds of
polar rain enhancement phenomena and the characteristics of solar wind, we selected
typical symmetric and asymmetric enhancement events from the data from August
12, 1978 to December 31, 1979.   The criteria for selecting the events were described
previously.   A total of 62 polar passes were selected as showing symmetric events,
and 148 polar passes were selected as showing asymmetric events.   On account of the
solar wind propagation time, the solar wind data were shifted by one hour to compare
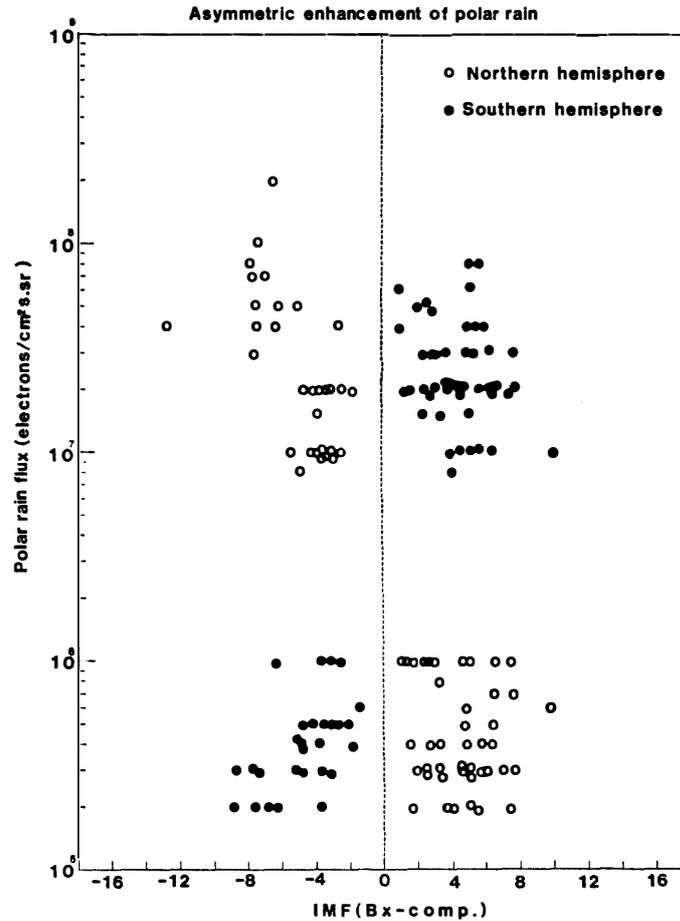
Fig. 5a.   Asymmetric enhancement of polar rain flux and the scattering of IMF Bx values.   It shows
that, for positive Bx values, the polar rain flux in the southern hemisphere is higher than
that in the northern hemisphere and, on the contrary, for negative Bx values, the polar
rain flux in the northern hemisphere is higher than that in the southern hemisphere.

them with the low-altitude DMSP satellite data.   Figures 5a and 5b show the statistical
relationships between the scattering of IMF Bx values and the flux of polar rain for
symmetric and asymmetric events.

The left and right panels show asymmetric and symmetric cases of polar rain
enhancement, respectively.   For the asymmetric cases, when Bx is positive, the polar
rain flux in the southern hemisphere is always higher than that in the northern hemi-
sphere.   On the contrary, when Bx is negative, the polar rain flux in the northern
hemisphere is higher than that in the southern hemisphere.   These results suggest
that the sunward magnetotail field lines in the northern polar cap interact with the
anti-sunward IMF component $(Bx<0)$ and the anti-sunward magnetotail field lines in
the southern polar cap interact with the sunward IMF component $(Bx>0)$.

For the symmetric cases shown in Fig. 5b, no clear relationship is found between
the enhancement of northern or southern polar rain flux and the IMF Bx polarity.
Absolute values of Bx in the symmetric enhancement of polar rain seem to be more
scattered than those in the asymmetric enhancement of polar rain.

Since symmetric enhancement of polar rain is frequently observed during the
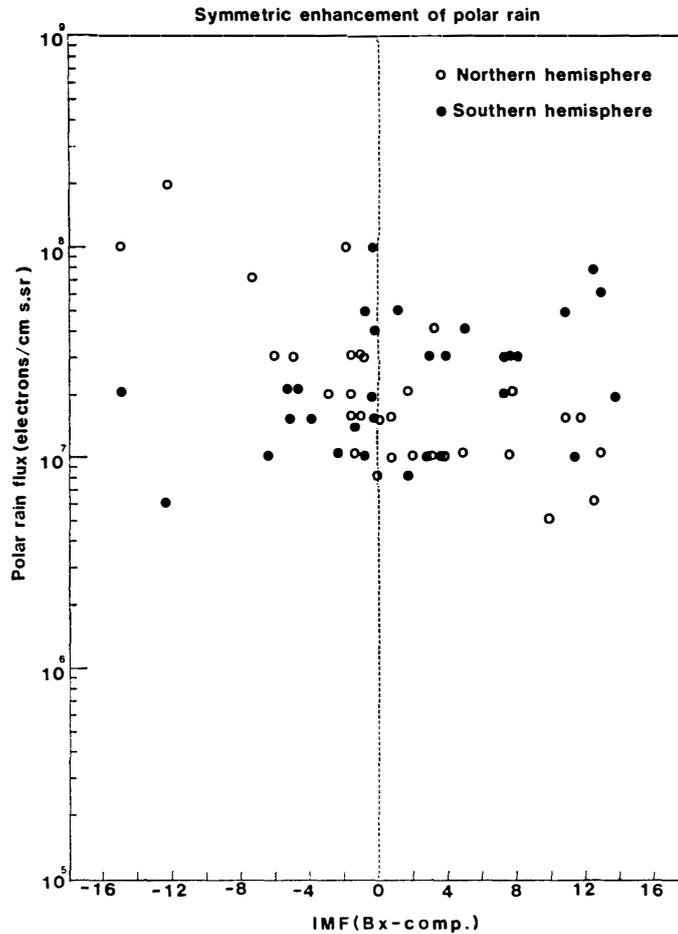
Fig. 5b. Symmetric enhancement of polar rain flux and the scattering of IMF Bx values. There
is no clear relationship between the IMF Bx polarity and the polar rain flux in the northern
or the southern hemisphere.

period when the polarity of the IMF *Bx* component is fluctuating, as shown in Fig. 2,
IMF in these cases may interact with magnetotail field lines in both polar caps.

We also examined the dependence of particle flux on the polarity of IMF *By* for
asymmetric and symmetric cases.   Figures 6a and 6b show the statistical relationship
between the scattering of IMF *By* values and the flux of polar rain for both cases.   For
the case of the asymmetric enhancement of polar rain in Fig. 6a, when *By* is positive,
most of the polar rain flux in the northern hemisphere is higher than that in the southern
hemisphere except several events.   On the contrary, when *By* is negative, the polar
rain flux in the southern hemisphere is higher than that in the northern hemisphere.

Generally, IMF has two different kinds of sector structures, IMF $By<0$ and
IMF $Bx>0$ in the toward sector and IMF $By>0$ and IMF $Bx<0$ in the away sector.
Thus, the IMF $Bx>0$ period generally corresponding to the IMF $By<0$ period and
vice versa.   However, it should be noted that there are several exceptional cases,
which do not follow the general relationship between the IMF *By* polarity and the
asymmetric enhancement of polar rain.   The comparison of Figs. 5a and 5b suggests
that the asymmetric enhancement of polar rain is more strongly controlled by the IMF
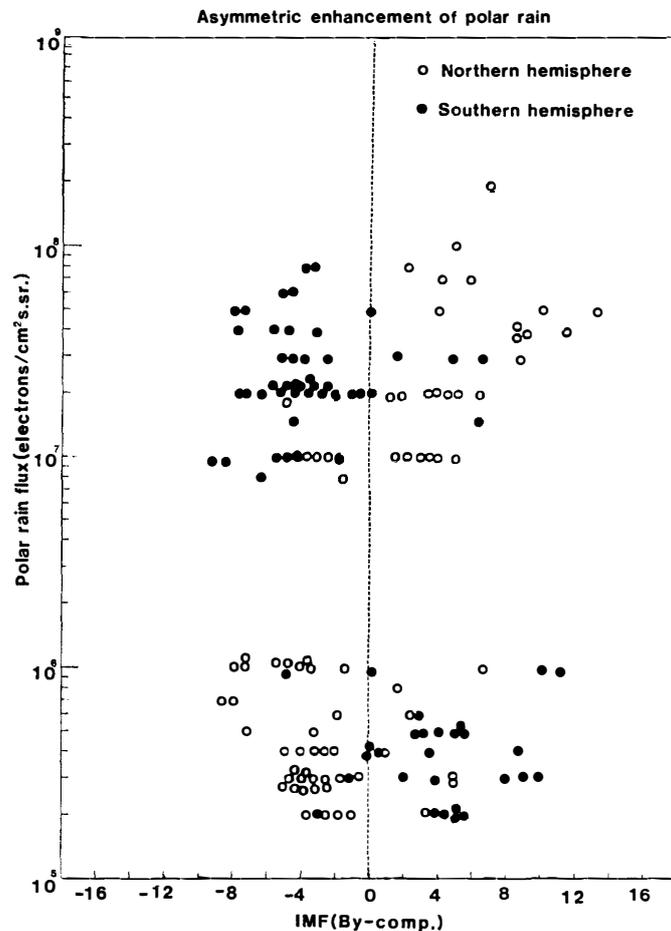
Fig. 6a.   Asymmetric enhancement of polar rain flux and the scattering of IMF By values. Polar rain flux in the northern hemisphere is mostly higher than that in the southern hemisphere for positive By values and, on the contrary, for negative By values, polar rain flux in the southern hemisphere is mostly higher than that in the northern hemisphere.   It should be noted that there are several exceptions to the relationship between the IMF By polarity and the hemisphere of polar rain enhancement.

Bx polarity than by the IMF By polarity.

For the case of the symmetric enhancement of polar rain shown in Fig. 6b, no clear relationship is recognized between the enhancement of northern or southern polar rain flux and the IMF By polarity.   Large By scattering can be seen in this event.

4. Summary and Discussion

From the examination of DMSP electron precipitation data, it is found that there are two types of intense electron precipitation phenomena over the polar cap.   They are the symmetric and asymmetric enhancement of polar rain.   These two types of precipitation occur under different IMF conditions.   The results are summarized as follows:

For symmetric enhancement of polar rain phenomena;
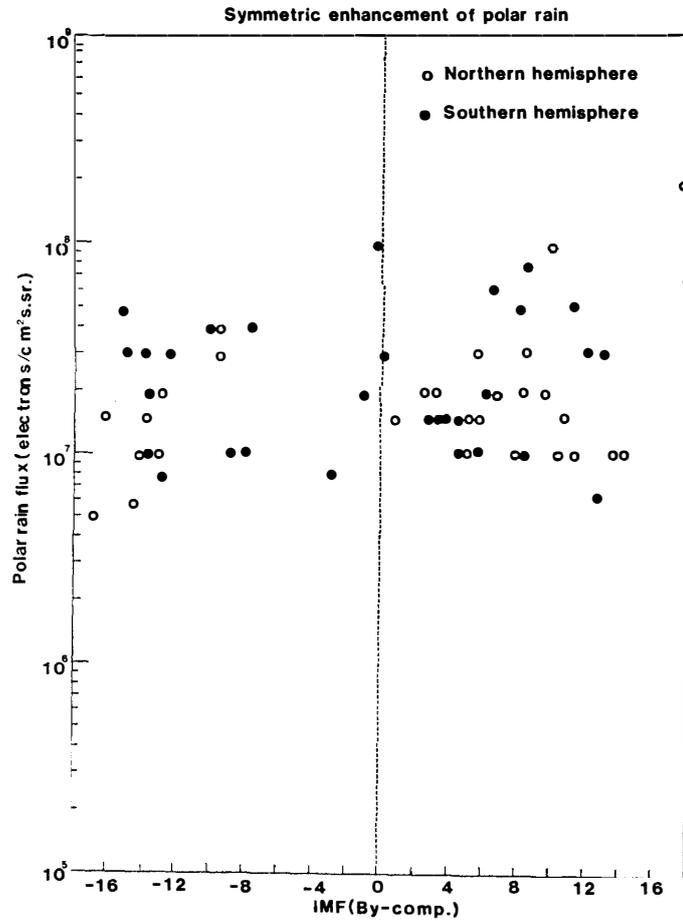
Fig. 6b.   Symmetric enhancement of polar rain flux and the scattering of IMF By values.   There
is no clear relationship between the IMF By polarity and the polar rain flux in the northern
or the southern hemisphere.

(1)   There is no clear correlation between the occurrence of this event and the
IMF Bx and By polarities.

(2)   IMF Bx and By components show fluctuations during the occurrence period.

(3)   Most of these phenomena seem to be related to the sudden storm commence-
ment.

For asymmetric enhancement of polar rain phenomena;

(1)   There is a very clear correlation between the north-south asymmetry of this
event and the polarity of IMF Bx component.   Enhancement of polar rain flux in the
southern hemisphere is seen during the positive IMF Bx period and enhancement of
polar rain flux in the northern hemisphere is seen during the negative IMF Bx period.
The correlation between the IMF By component and the north-south asymmetry of
polar rain flux is also recognized.   However, there are several exceptions.   It is con-
cluded that the IMF Bx polarity mainly controls the north-south asymmetric enhance-
ment of polar rain.

(2)   IMF Bx and By components are stable polarity during this type of event.

(3)   These events may not be directly related to the sudden storm commencement.

We also examined the relationship between the occurrence of these two types of

enhancement and the characteristics of the solar wind density, velocity and temperature. It is found that the solar wind proton density during the symmetric event is usually higher than that during the asymmetric events. We consider that symmetric enhancement of polar rain is caused by the arrival of solar wind shock wave at the magnetosphere. Through the interaction between IMF and both the northern and the southern magnetotail field lines, solar wind electrons may be accelerated and precipitate to the low-altitude polar cap regions.

On the other hand, asymmetric enhancement of polar rain clearly depends on the IMF sector structure. We concluded that the polarity of IMF Bx, rather than that of By, significantly controls the north-south asymmetry in the polar rain enhancement. This fact suggests that the anti-parallel magnetic merging (between magnetospheric field lines and IMF) is important in controlling the polar rain particle flux. We further examined the seasonal variation of these events and found that the asymmetric enhancement of polar rain was mostly observed in the summer hemisphere. This fact indicates that the strength of interaction between IMF and anti-parallel magnetotail field line depends on the geometrical relation between the solar wind and the earth's magnetosphere. On the other hand, the seasonal variation of polar rain symmetric enhancement was not clearly recognized in our analysis. More detailed examination of these problems will be reported in a separate paper.

References

BURCH, J. L., FIELDES, S. A. and HEELIS, R. A. (1979): Polar cap electron acceleration regions. J. Geophys. Res., **84**, 5863–5874.

CAMPBELL, W. H. and MATSUSHITA, S. (1973): Correspondence of solar field direction and polar cap geomagnetic field changes for 1965. J. Geophys. Res., **78**, 2079–2087.

DUNGEY, J. W. (1961): Interplanetary magnetic field and the auroral zones. Phys. Res. Lett., **6**(2), 47–52.

HARDY, D. A., GUSSENHOVEN, M. S. and HUBER, A. (1979): The precipitation electron detectors (SSJ/3) for the block 5D/flight 2–5 DMSP satellites; Calibration and data presentation. Rep. AFGL-TR-79-0120, Air Force Geophys. Lab., Hanscom Air Force Base, Bedford.

MENG, C.-I. and KROEHL, H. W. (1977): Intense uniform precipitation of low energy electrons over the polar cap. J. Geophys. Res., **82**, 2305–2313.

SVALGAARD, L. (1973): Polar cap magnetic variations and their relationship with the interplanetary magnetic sector structure. J. Geophys. Res., **78**, 2064–2078.

WINNINGHAM, J. D. and HEIKKILA, W. J. (1974): Polar cap auroral electron fluxes observed with ISIS 1. J. Geophys. Res., **79**, 949–957.

YEAGER, D. M. and FRANK, L. A. (1976): Low energy electron intensities at large distances over the earth's polar cap. J. Geophys. Res., **81**, 3966–3976.